Transactions of the Korean Nuclear Society Spring Meeting
Jeju, Korea, May 10-11, 2007

Error Reduction of the Axial Kernel of the DeCART Code

Jin-Young Cho,a Kang-Seog Kim,a Chung-Chan Lee,a Sung-Quun Zee,a Han-Gyu Joo b
Korea Atomic Energy Research Institute, 150 Deokjin-dong, Yuseong-gu, Daejon, 305-353, jyoung@kaeri.re.kr
b Department of Nuclear Engineering, Seoul National University, San 56-1, Sillim-dong, Kwanak-gu, Seoul, 151-742

1. Introduction

Recently, an error quantification [1] for the axial kernel of the DeCART code was performed for a demonstrative problem, and it revealed that the homogenization error is negligible, but the diffusion and the nodal errors are greater than 100 pcm. This paper introduces a SP_3 approximation [2] to reduce the diffusion error, and a SANM solution [3] and a sub-plane scheme to reduce the nodal error. The proposed approaches are examined for the demonstrative problem and the C5G7MOX 3-D extension problems [4].

2. Axial Solution integrated CMFD Equation

The nodal neutron balance equation for a CMFD formulation used in the DeCART code can be written for a homogenized node (l,k) as:

$$\frac{1}{h_{rad}}\sum_{s=1}^{N_{rad}^{l}} J_{rad}^{l,k,s} + \frac{1}{h_z}\sum_{s=1}^{N_z^k} J_z^{l,k,s} + \Sigma_r^{l,k}\bar{\phi}^{l,k} = \bar{S}^{l,k}, \qquad (1)$$

where $J_{rad}^{l,k,s}$, $J_z^{l,k,s}$, $\bar{\phi}^{l,k}$ and $\bar{S}^{i}$ are the net currents to the radial and the axial surfaces, the node averaged flux and the source including the fission and the scattering, and N_{rad}^{l} and N_z^k are the number of neighboring nodes for the radial and the axial directions, respectively.

The radial net current in the CMFD formulation can be written as:

$$J_{rad}^{l,k,R} = -\tilde{D}^{l,k,R}\left(\bar{\phi}^{l+1,k} - \bar{\phi}^{l,k}\right) - \hat{D}^{l,k,s}\left(\bar{\phi}^{l+1,k} + \bar{\phi}^{l,k}\right), \qquad (2)$$

where $\tilde{D}^{l,k,R}$, $\hat{D}^{l,k,R}$ are the coupling term of the ordinary finite difference method (FDM) and the current corrective term, respectively.

3. Systematic Error Reduction

3.1. Reduction of Nodal Error

A nodal error originates mainly from: (1) an inaccurate flux shape approximation and (2) an inaccurate transverse leakage approximation. The error resulting from the flux shape approximation can be resolved by introducing the higher order nodal solution of SANM of Ref. 3 or a sub-plane scheme where the MOC plane is divided into multiple nodal planes. The error resulting from the transverse leakage approximation can be resolved by introducing an accurate transverse leakage model.

In the sub-plane method, multiple planes to obtain the radial CMFD and the axial nodal solutions are defined within the thick MOC planes. The planar MOC calculation is only performed at the thick MOC planes to produce the cell homogenized cross sections of Eq. (1) and the current corrective term of Eq. (2). Multiple planes that belong to a MOC plane use the same homogenized cross sections and current corrective terms. Eq. (1) is solved for all the sub-planes and the radial nodes. Table 1 shows the solution errors of the sub-plane scheme from the conventional multi-plane schemes for the IM case of the demonstrative problem. This Table shows that the sub-plane scheme produces almost the same solution as the conventional multi-MOC plane scheme with lesser computing time than the conventional scheme.

Table 1. Solution Errors of the Sub-Plane Scheme for the IM Case of the Demonstrated Problem

N_{sp} [1)]	keff Error[2)], pcm	Power Error, %	CPU Time Ratio[3)]
2	-6.3	-0.01	0.534
5	-0.3	-0.02	0.214
10	-0.2	-0.03	0.046

1) Number of sub-planes per MOC plane
2) Reference: the conventional multi plane scheme
3) Relative computing time of the sub-plane scheme to the conventional scheme

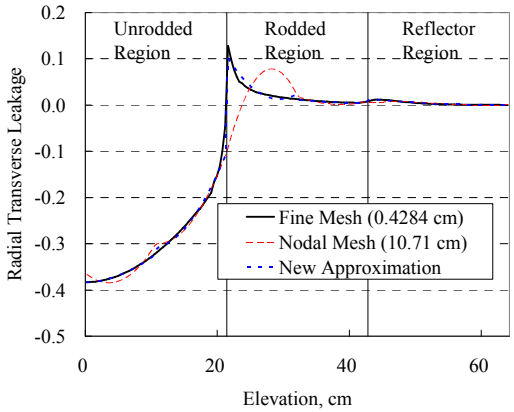

Fig. 1 Pin-level radial leakage axial profile

The conventional NEM approximates the 1-D transverse leakage shape by using the three transverse leakages of a node average and two surface values. This approximation has been successful for an assembly-based nodal calculation because the transverse leakage varies smoothly between the nodes. However, as shown in Fig. 1 for the pin calculation, the transverse leakage varies sharply at the interface between the unrodded and the rodded nodes. In this case, the transverse leakage

shape from the conventional approximation which is noted by a red line in Fig. 1 is not valid. Therefore, a new scheme for a pin-based transverse leakage by using the intra-nodal flux shape is proposed. In the proposed scheme, the second order transverse leakage shape is obtained from the three partly averaged transverse leakages which are achieved by using the partly averaged fluxes and Eq. (2). The proposed transverse leakage shape which is also noted by a blue line in Fig. 1 follows the reference shape well.

3.2. Introduction of a SP_3-NEM solution

The odd-order outgoing partial moments at the surfaces of node (*l,k*) can be manipulated as:

$$\mathbf{J}^{l,k,o} = \mathbf{T}_1^{l,k}\mathbf{J}^{l,k,i} + \mathbf{T}_2^{l,k}\mathbf{X}^{l,k} + \mathbf{T}_3^{l,k}\mathbf{Z}^{l,k}, \qquad (3)$$

where

$$\mathbf{J}^{l,k,o} = \left[J_1^{l,k,T,o} \quad J_1^{l,k,B,o} \quad J_3^{l,k,T,o} \quad J_3^{l,k,B,o}\right]^T,$$

$$\mathbf{J}^{i} = \left[J_1^{l,k,T,i} \quad J_1^{l,k,B,i} \quad J_3^{l,k,T,i} \quad J_3^{l,k,B,i}\right]^T,$$

$$\mathbf{X}^{l,k} = 20\left[\overline{\Phi}_{00}^{l,k} \quad \overline{\phi}_{20}^{l,k}\right]^T - 70\left[\widetilde{\Phi}_{02}^{l,k} \quad \widetilde{\phi}_{22}^{l,k}\right]^T,$$

$$\mathbf{Z}^{l,k} = 30\left[\widetilde{\Phi}_{01}^{l,k} \quad \widetilde{\phi}_{21}^{l,k}\right]^T,$$

$$\overline{\Phi}_{00}^{l,k} = \overline{\phi}_{00}^{l,k} + 2\overline{\phi}_{20}^{l,k},\ \widetilde{\Phi}_{02}^{l,k} = \widetilde{\phi}_{02}^{l,k} + 2\widetilde{\phi}_{22}^{l,k}.$$

The two subscripts of the angular moments in Eq. (3) mean the angular and spatial orders. The governing equations can be derived by inserting Eq. (3) to Eq. (1).

In solving the SP_3 equation, the nodal balance equation for the second order angular moment is also required such as Eq. (1). The radial current for this second order equation is approximated by using the finite difference method rather than CMFD.

4. Benchmark Calculation

Tables 2 and 3 show the computational results for the newly implemented features of the DeCART axial kernel. The final solution for the diffusion calculation can be obtained by using 5 sub-planes which contain a negligible nodal error. The newly implemented transverse leakage scheme shows less nodal errors than the conventional scheme when comparing the solutions of one sub-plane with those of 5 sub-planes. The SANM solutions when using one sub-plane and the newly implemented transverse leakage scheme show less nodal errors than the NEM solutions. Table 1 also shows that the final diffusion solutions contain more than 100 pcm of diffusion errors. These diffusion errors on the eigenvalue can be reduced considerably by introducing the SP_3 equations. The pin power error is also reduced by introducing the SP_3 equations, but the effects are less than those on the eigenvalue. The final solution of the DeCART code for this benchmark problem shows less than 30 pcm of an eigenvalue and 2 % of local pin power errors.

5. Conclusion

In this paper, the SANM solution, sub-plane scheme and a new transverse leakage approximation were introduced to reduce the axial nodal error and the SP_3-NEM solution was introduced to reduce the diffusion error of the DeCART code. The benchmark calculation showed that the newly implemented axial solvers eliminated most of all the nodal and diffusion errors.

Table 2. Solution Errors of DeCART Diffusion Kernel for C5G7MOX 3-D Extension Problem

Problems	TL	Nsp[1]	Nodal	Err-k[2]	Err-P[3]	Err-P[4]
Unrod	Conv.	1	NEM	-63.8	1.88	0.78
			SANM	-6.2	3.81	0.74
		5	Both	95.4	1.92	0.72
	New	1	NEM	-157.5	4.65	0.84
			SANM	-101.1	2.18	0.71
		5	Both	-99.5	1.99	0.70
		5	Both	-99.4	1.60	0.68
Rodded Conf. B	Conv	1	NEM	4.5	5.95	0.72
			SANM	-43.6	3.33	1.13
		5	Both	-182.1	2.28	1.40
	New	1	NEM	-163.3	2.48	1.07
			SANM	-160.7	1.98	1.24
		5	Both	-175.9	2.19	1.35

2) Eigenvalue Error, pcm
3) Maximum local pin power error, %
4) Maximum axially integrated pin power error, %

Table 3. Solution Errors of DeCART SP_3 Kernel for C5G7MOX 3-D Extension Problem

Problems	TL	Nsp[1]	Err-k[2]	Err-P[3]	Err-P[4]
Unrod	Conv.	1	12.2	1.75	0.84
		5	-14.4	1.65	0.76
	New	1	-75.0	4.47	0.82
		5	-19.6	1.77	0.75
Rodded Conf. A	Conv.	1	95.7	2.80	1.11
		5	-11.0	1.80	0.74
	New	1	-29.6	4.66	1.09
		5	-9.8	1.84	0.77
Rodded Conf. B	Conv.	1	147.2	7.69	0.81
		5	-40.8	1.41	0.95
	New	1	-19.9	3.90	0.69
		5	-31.4	1.49	0.87

REFERENCES

[1] J. Y. Cho, et al., "Error Quantification of the Axial Nodal Diffusion Kernel of the DeCART cCode," PHYSOR 2006, Vancouver, B.C., Canada, 2006.
[2] C. H. Lee and T. J. Downar., "A Hybrid Nodal Diffusion/SP_3 Method Using One-Node Coarse-Mesh Finite Difference Formulation," Nucl. Sci. Eng. 146, 176, 2004.
[3] T. Y. Han, et al.., "Two-Group CMFD Accelerated Multi-Group Calculation with a Semi-Analytic Nodal Kernel," PHYSOR 2006, Vancouver, B.C., Canada, 2006.
[4] M. A. Smith, et al., "Benchmark on Deterministic 3-D MOX Fuel Assembly Transport Calculation without Spatial Homogenization," Progress in Nuclear Energy. 48, 383, 2006.